Ocean Dynamics (2004) 54: 477–488
DOI 10.1007/s10236-004-0093-8

Bjørn Gjevik · Roger A. Flather · Daniel Hareide

Sea-level oscillations with 6-h period in the North Sea 29–31 October 2000. An analysis of data from stations in the northern North Sea and along the western coast of Norway

Received: 7 January 2004 / Accepted: 25 February 2004

Abstract During the storm event 29–31 October 2000 long regular trains of residual sea-level oscillations with period about 6 h occurred in the North Sea area. Crest-to-trough heights up to 0.8 m were observed along the western coast of Norway. Model simulations show that these oscillations were mainly due to spatial and temporal variations in the atmospheric forcing and were not the result of nonlinear tide–surge interaction. The oscillations propagated northwards along the Norwegian coast and the signal was amplified in some fjords in agreement with predictions by high-resolution regional models. In Skagerrak in the north eastern North Sea the main storm-surge signal appeared as amplitude-modulated oscillations with period about 12 h and crest-to-trough height up to 1.5 m. Here the tide–surge interaction contributed up to about 20% of the peak surge. On the coast of Scotland and in the southern part of the North Sea nonlinear effects produced oscillations with 6-h period at some stations.

Keywords Sea level oscillations · Quarter diurnal · North Sea · Norwegian coast

1 Introduction

Sea-level oscillations in the quarter-diurnal band, i.e., period about 6 h, are primarily generated by nonlinear distortion of the semidiurnal tide in shallow waters. In the North Sea area it is well documented that the dominant semidiurnal M_2 tide in some regions leads to a significant quarter-diurnal overtide (M_4) due to nonlinear effects, namely, advection, wave drift, quadratic bottom friction, and time-dependent viscosity. The amplitude and phase of the M_4 tide in the North Sea is mapped by models and compared with in situ sea-level measurements by Davies (1986), Kwong et al. (1997), and also by satellite altimetry Andersen (1999). The largest sea-level amplitudes, up to 25 cm, are found in the southern parts of the North Sea and in the English Channel. In the Irish Sea the M_4 tide has been modeled by Davies and Jones (1996) with sea-level amplitudes up to 20 cm in the Liverpool Bay and Morecambe Bay regions in the eastern part of the sea. The M_4 tide shows relatively rapid spatial variation in amplitude and phase and is localized to limited areas basically in shallow water.

Possible transient generation of sea-level oscillations in the M_4 band due to interaction between the M_2 tide and wind-generated current was inferred by Pingree et al. (1984) and Davies and Lawrence (1994) from model studies, but has, to our knowledge, not been documented by observations.

A strong storm event in late October 2000 generated a large storm surge, particularly in the northeastern part of the North Sea and in Skagerrak. Superimposed on the main surge signal, an unusual sequence of residual sea-level oscillation with period about 6 h was recorded in the North Sea area. Particularly along the western coast of Norway, outside the main storm area, long trains of oscillations with period about 6 h and amplitude up to 0.8 m are evident in the observations. Oscillations with period around 6 h were also observed on the south-western coast of Denmark and along the coast of Great Britain (Flather and Williams 2001). At some stations, particularly in the northeastern part of the North Sea and in Skagerrak, the main storm surge signal was dominated by a group of amplitude-modulated oscillations with period around 12 h and peak-to-peak amplitude range up to 1.5 m.

Responsible Editor: Gerd Becker

B. Gjevik (✉)
Department of Mathematics, University of Oslo,
P.O. Box 1053, Blindern, 0316 Oslo, Norway.
e-mail: bjorng@math.uio.no

R. A. Flather
Proudman Oceanographic Laboratory,
Birkenhead, CH43 7RA, UK

D. Hareide
The Norwegian Hydrographic Service, Stavanger

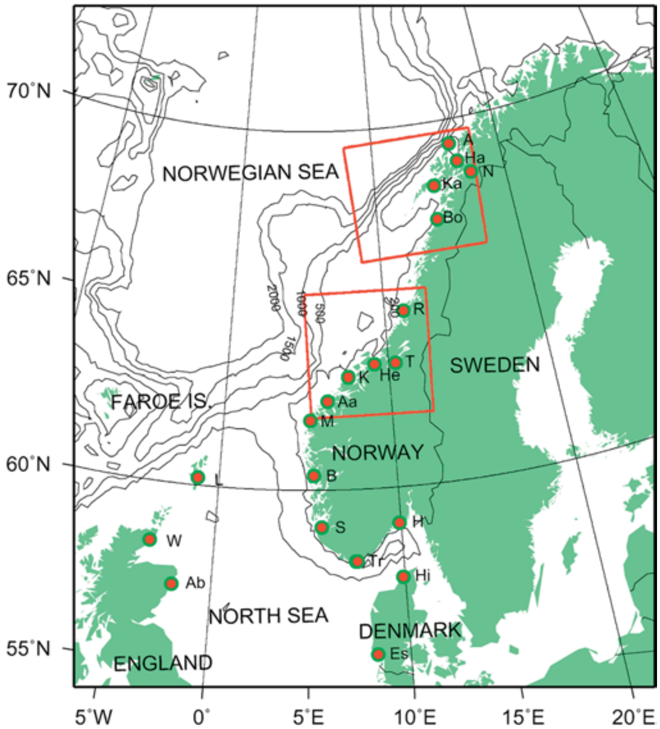

Fig. 1 Map of the northern part of the North Sea and the western coast of Norway. Stations with sea-level records are marked with *map code* (see Table 1). *Rectangles* mark the domains for the high-resolution models around the Lofoten Islands (northern) and mid-Norway (southern). Depth contours in meters

Table 1 List of stations with sea-level records

Station	Coordinates	Map code
Esbjerg	55°28′ N, 08°27′ E	Es
Hirtshals	57°36′ N, 09°58′ E	Hi
Helgeroa	59°00′ N, 09°52′ E	H
Tregde	58°00′ N, 07°34′ E	Tr
Stavanger	58°58′ N, 05°44′ E	S
Aberdeen	57°09′ N, 02°04′ W	Ab
Wick	58°26′ N, 03°05′ W	W
Lerwick	60°09′ N, 01°08′ W	L
Bergen	60°24′ N, 05°18′ E	B
Måløy	61°56′ N, 05°07′ E	M
Ålesund	62°28′ N, 06°09′ E	Aa
Kristiansund	63°07′ N, 07°45′ E	K
Heimsjø	63°26′ N, 09°07′ E	He
Trondheim	63°26′ N, 10°26′ E	T
Rørvik	64°52′ N, 11°15′ E	R
Bodø	67°17′ N, 14°23′ E	Bo
Narvik	68°26′ N, 17°25′ E	N
Kabelvåg	68°13′ N, 14°30′ E	Ka
Harstad	68°48′ N, 16°33′ E	Ha
Andenes	69°19′ N, 16°09′ E	A

During the same storm event, harbor seiching with period about 1.5 h was observed at the Port of Rotterdam in the southern North Sea and linked to the passage of a cold front on 30 October (de Jong et al 2003).

The occurrence of oscillations in the 6-h (M_4) band raises the question whether these oscillations are due to nonlinear coupling between the astronomic semidiurnal tide and the surge signal at nearly the same period. Another possible explanation is that the oscillations are primarily an effect of an unusual atmospheric forcing pattern combined with amplification in some Norwegian fjords after the sea-level signal has propagated out of the generation area.

This paper presents an analysis of sea-level records mainly from stations along the Norwegian coast and some adjacent stations on the coasts of Britain and Denmark in order to examine the properties of this unusual event and to investigate its generation mechanism. The map in Fig. 1 shows the geographical area of interest and the locations of the stations with sea-level observations (see also Table 1).

2 Meteorological data

The general weather situation during the late October 2000 event (Fig. 2) shows an extensive low-pressure system over the North Sea with secondary low-pressure centers precessing round each other. The minimum pressure was below 955 hPa for part of the period and pressure was below 980 hPa over large parts of the shelf.

Fig. 2 Weather map for 30 October 2000, 00 and 12 GMT. Isobars with 4-hPa intervals. (Courtesy of the Meterological Office, Bracknell, England)

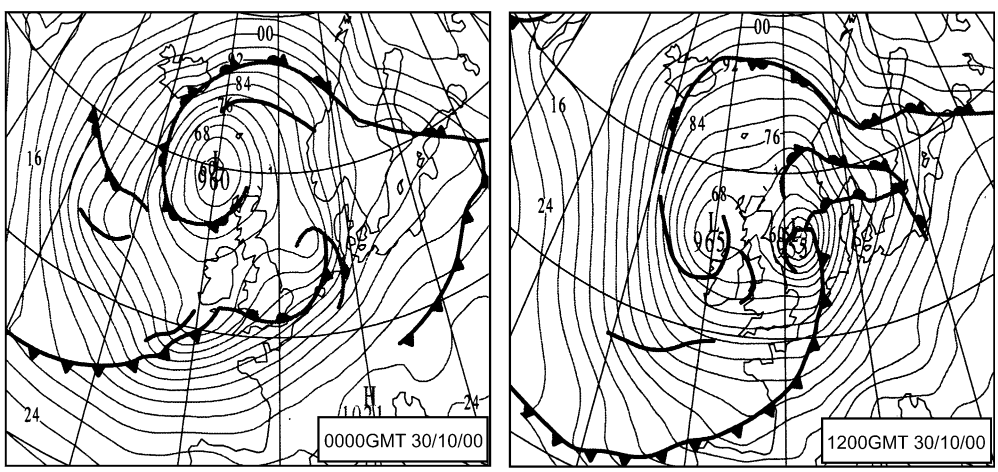

Associated with the low-pressure centers, strong wind occurred over the North Sea area and the multiple-pressure centers and fronts led to complex variations in wind speed and direction. An exceptionally strong storm center (Tora) hit the southern coast of Norway in the afternoon of 30 October. Associated with the passage of these storms and low-pressure centers, large sea-level variations were observed all around the North Sea.

Small-scale spatial and temporal variations in the wind field in the area west of Stavanger in southern Norway are clearly displayed by wind-stress maps (Fig. 3) plotted from data from the atmospheric model used to force the British operational storm-surge model CS3 (see Sect. 3). This picture is supported by wind observations from two stations (Obrestad and Utsira) on the coast near Stavanger and the offshore platform, Sleipner, South-West of Stavanger. The wind records were sampled with 1-h intervals at Utsira and Sleipner and 10-min intervals at Obrestad. The wind records from Obrestad lighthouse about 35 km southwest of Stavanger (Fig. 4) show a wind speed peak late on 30 October (at 42 h) corresponding to the exceptionally strong storm, Tora, which developed in the North Sea area. A smaller wind peak was observed about 12 h earlier (at 30 h). The wind observations from Utsira about 60 km northwest of Stavanger show four dominant oscillations in wind speed starting at 06 UTC 30 October (30 h) and lasting for about 24 h. The mean period of these oscillations is about 6 h. At the offshore platform Sleipner about 230 km South-West of Stavanger strong oscillation in wind speed was observed from about 30 October 12 UTC to 31 October 00 UTC. (36–48 h).

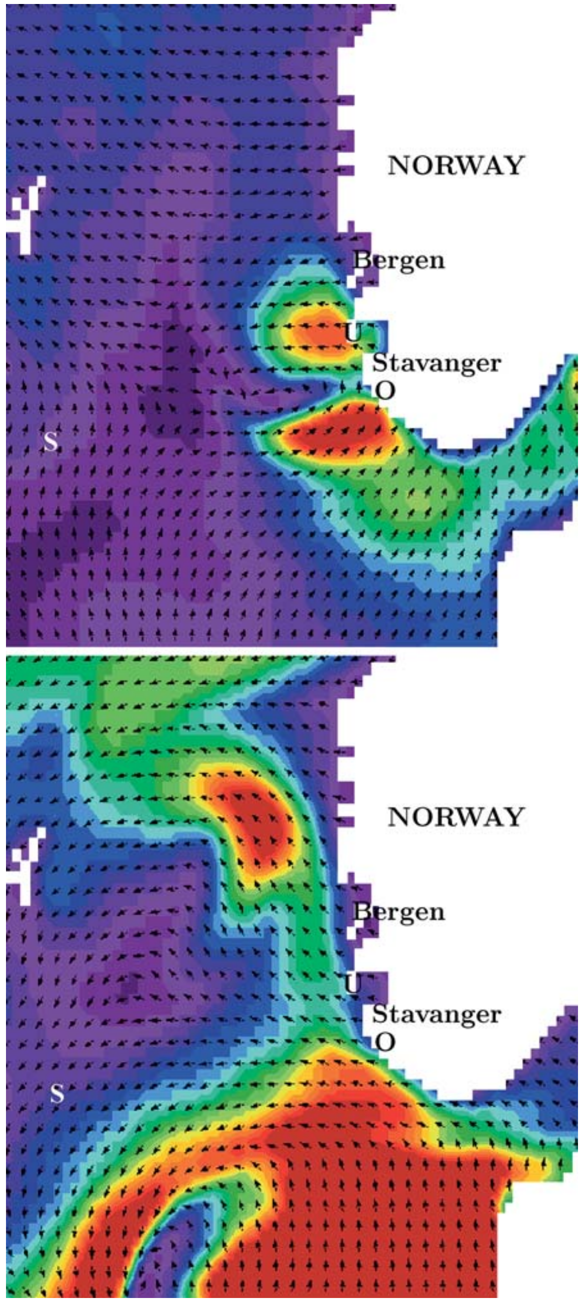

Fig. 3a, b Wind stress 30 October 2000, 06 UTC (**a**) and 12 UTC (**b**) from the atmospheric model used as forcing for the British operational storm surge model (CS3). *Color code* indicates strength of wind stress; *blue-green-yellow-red* represent low–high values. Letters *O*, *U*, and *S* mark the position of Obrestad, Utsira, and Sleipner respectively. *Arrows* show direction of wind stress

3 Models

Proudman Oceanographic Laboratory (POL) has developed and maintained tide-surge models run operationally in real-time at the UK Meterological Office since 1978. They produce surge predictions for use in the warning system for coastal floods in England and Wales. The current model, CS3, with resolution ~12 km was introduced in 1991 (Flather 2000). The model is forced by surface pressure and 10-m wind fields supplied hourly from the Met Office mesoscale weather forecast model (resolution also ~12 km). The surge models run four times per day, each run consisting of a 6-h hindcast, driven by met data including assimilated meteorological observations, and a 48-h forecast. Hourly model fields are archived for subsequent analysis. We used data from CS3 model runs for comparison with the recorded sea-level data from the period 29–31 October 2000 in Sections 4 and 5.

In order to investigate the propagation of the sea-level signal along the coast of Norway, we also performed a series of specially designed model simulations. First, a regional barotropic tidal model for the Norwegian–Barents Seas (Gjevik et al. 1994), refined to 12.5-km resolution, was modified to allow specified wave input at a southern boundary section at about 58 °N from Stavanger, southern Norway, to Aberdeen in Scotland. The volume flux normal to the boundary was set to;

$$V(s,t) = \frac{a\sqrt{gh}}{L}(L-s)\alpha t \exp(1-\alpha t)\sin(2\pi\frac{t}{t_p}), \qquad (1)$$

Fig. 4 Observed wind speed (*full line*) and direction in degree true (*dotted line*) at three stations: *Sleipner, Obrestad,* and *Utsira*. Time origin 00 UTC 29 October 2000

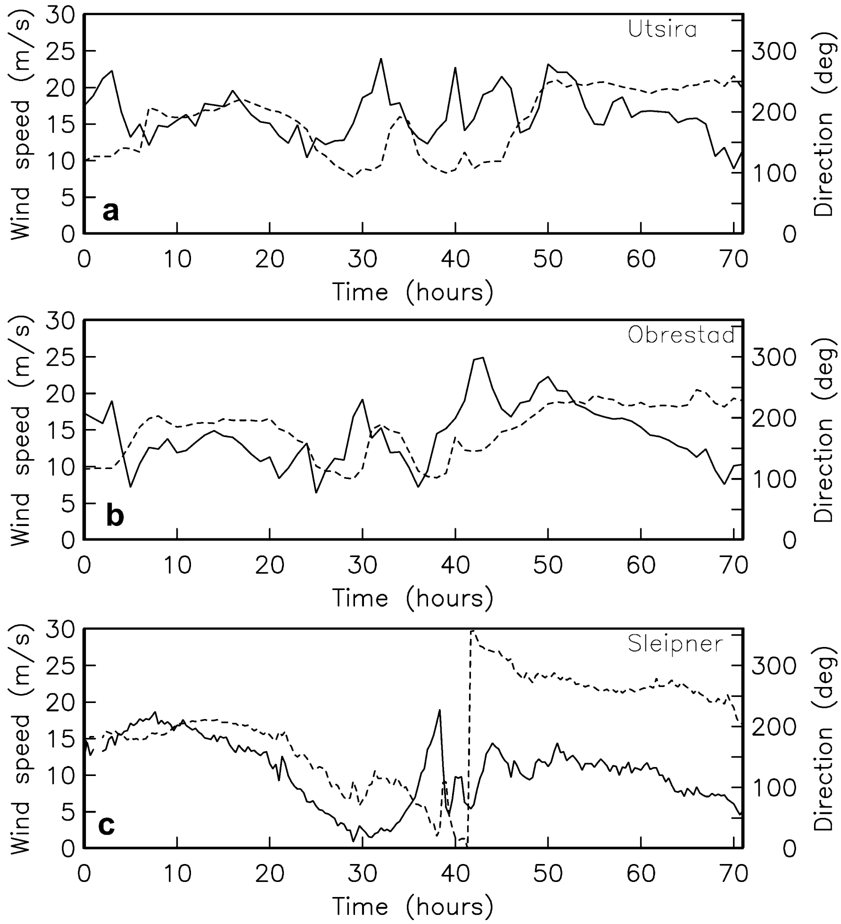

where s is the distance from the coast at Stavanger, t is time, L is the length of the boundary section, $a = 0.1$ m is the sea-level amplitude of the wave, h is the depth, which is a function of s, and g is the acceleration of gravity. The duration of the wave group is set by the parameter α with $\alpha^{-1} = 24$ h, and the period of the individual waves $t_p = 6$ hours. Along the other open boundaries towards the North Atlantic and in the Arctic Ocean, radiation boundary conditions were used. We refer to this model as the NBS model and results of the simulations with it are described in Section 5.

The local wave transformation near the Lofoten Islands in northern Norway and in the Trondheimsfjord area in mid-Norway have been modeled with modified versions of the high-resolution barotropic tidal models with 500-m grid resolution for these regions (Moe et al. 2002, 2003). The location of the model domains is shown on the overview map in Fig. 1. We will subsequently refer to these models as HRN (northern) and HRS (southern), respectively. A method is applied for forcing the models similar to that for the NBS model above. This implies specified boundary input along the southern boundaries of the model domains and radiation boundary conditions on the western and northern boundaries. More details are given in Section 5, where the result of the simulations is presented and compared with the observations.

4 Sea level data

Sea-level data from 20 stations along the Norwegian coast and the neighboring coasts of the northern and northeastern parts of the North Sea and Skagerrak (Fig. 1 and Table 1) have been analyzed.

The stations along the Norwegian coast are operated by the Norwegian Hydrographic Service, Stavanger. The records were sampled with 10-min interval and for most stations harmonic constants for sea-level elevation, determined from long series of measurements, are available for an accurate detiding of the records. Data from the British stations with 15-min sampling intervals are made available from POL. The data from the two Danish stations are from the Danish Meteorological Institute and are also with 15-min sampling intervals.

In addition to data from the stations listed in Table 1, we also had access to records from several other stations along the coasts of Great Britain and one station at the Faroe Islands. After subtracting the predicted astronomical tide from the observed sea-level records, the residual signal from several stations shows an unusual series of sea-level oscillations during the period 29–31 October 2000.

The observed residual sea-surface displacement for the stations is plotted in Figs. 5 and 6. Predictions of

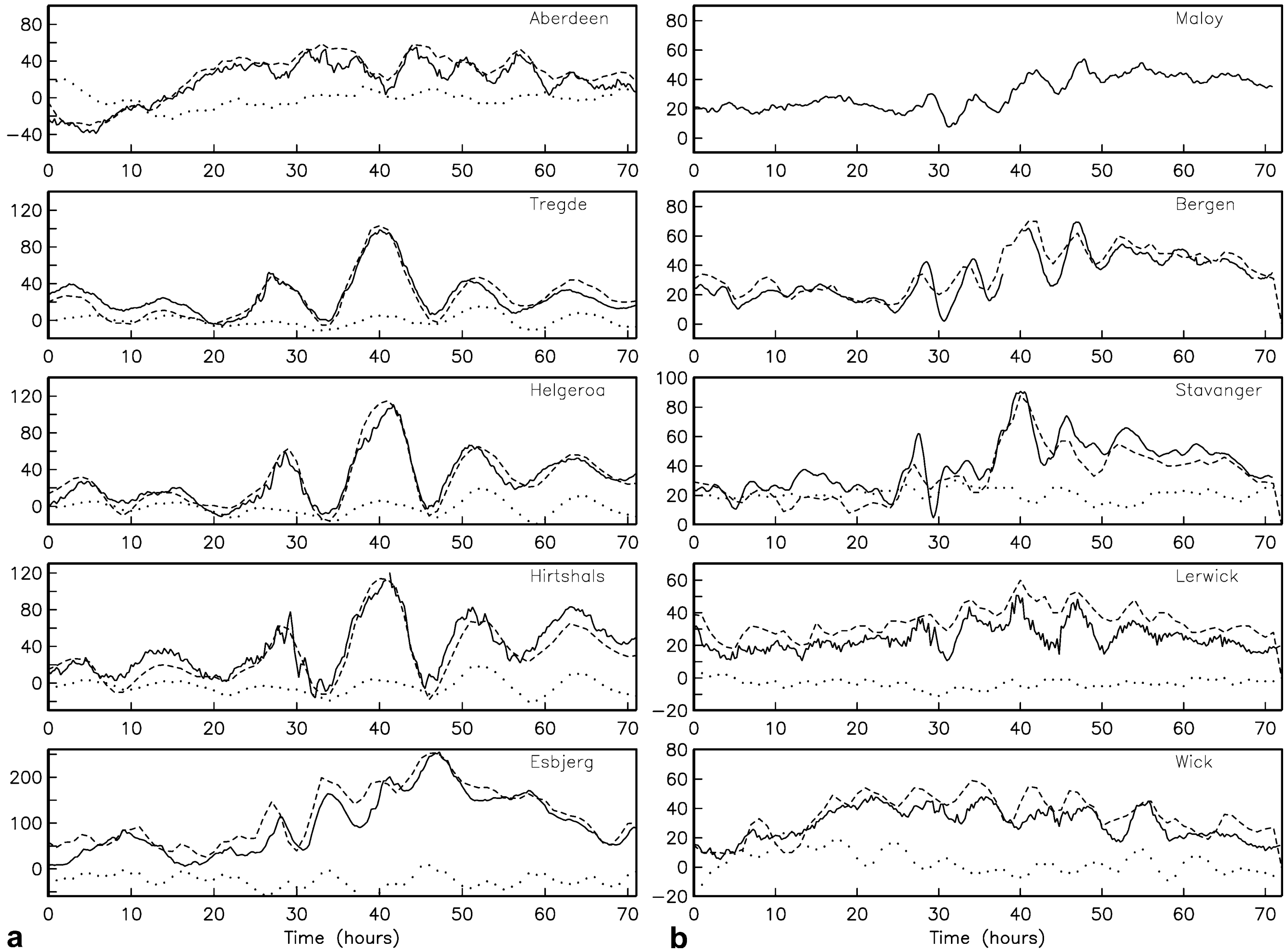

Fig. 5 Observed residual sea-surface displacement (in cm) for southern stations as function of time (*full lines*). Predicted residuals by CS3 model with tide included in the simulations (*broken lines*); *fine dotted lines* tide–surge interaction (see text). Time origin 00 UTC 29 October 2000

residual sea-surface displacement from the CS3 model (see Sect. 3) for some of the stations are shown on the corresponding plots. The three stations around Skagerrak in the northeastern North Sea (Hirtshals, Helgeroa, and Tregde, Fig. 5) show mainly a semidiurnal variation of the surge with period about 12.2 h and amplitude peaking in the afternoon of 30 October. At Tregde this occurred close to the time of the high tide and the sea level reached a record height of 115 cm above mean sea level. The astronomical tidal range is small in this area due to its proximity to the amphidromic point located between Tregde and Stavanger and the mean tidal range at Tregde at springs is 22.8 cm. The predictions by the CS3 model are in very good agreement with the observations for all three stations.

Aberdeen on the Scottish coast, across the North Sea west of Tregde, shows oscillations in sea level with period about 6 h on 30 and 31 October. Esbjerg on the southern part of the west coast of Jutland also shows short periodic oscillations, with period about 6 h, which are reproduced quite well by the CS3 model. It is interesting to note that the main four oscillations on 30 October (between 24 and 48 h, Fig. 5) correlates well with the main group of 6-h oscillations at Bergen. (Fig. 5), without any significant time delay.

On the Norwegian coast at Stavanger and Bergen (Fig. 5) the signal is dominated by oscillations with period about 6 h which for both stations also appear clearly in the model predictions. Oscillations with period about 6 h are also pronounced in the record from Lerwick on the Shetland Islands west of Bergen, and to a lesser extent at Wick on the Scottish coast. Records from the Faroe Islands west of Shetland (not shown here) show no clear evidence of oscillations with period about 6 h. This indicates that the signal has originated in the North Sea and had not propagated into the area from the North Atlantic north of Shetland. The main group of oscillations with period 6 h observed at Bergen propagated northwards along the western Norwegian coast and is clearly identified at Måløy (Fig. 5) and subsequently at Ålesund, Kristiansund, and Heimsjø (Fig. 6). At Trondheim, located in the long fjord northeast of Heimsjø, the oscillations are amplified, producing a long train of very regular oscillations on the 29–31 October. The period and amplitude of the oscil-

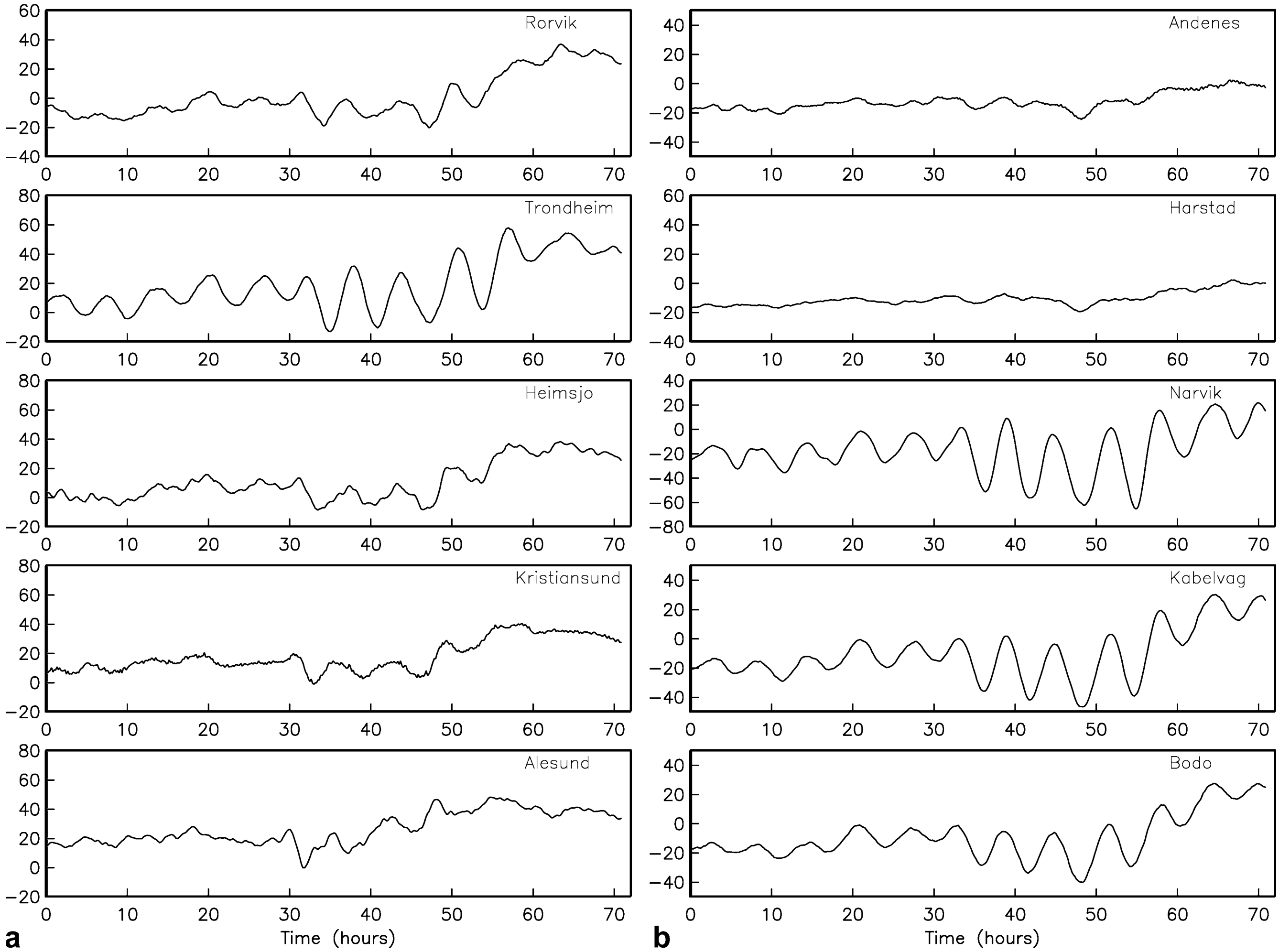

Fig. 6 Observed residual sea-surface displacement (in cm) for northern stations as function of time (*full lines*). Time origin 00 UTC 29 October 2000

lations are determined manually from the plot of the time series and checked with a spectral analysis. The period is found to be 6.1 h and the crest-to-trough height of the signal is up to 60 cm. At Rørvik, on the coast north of Trondheim, the signal is more blurred, but the main group of oscillations can still be identified. The stations north of Rørvik in the Lofoten area, Bodø, Kabelvåg and Narvik (Fig. 6) show regular trains of oscillations which are amplified in Vestfjorden, the large bay area located south of the Lofoten Islands (Fig. 9) .

The oscillations are most pronounced at Narvik at the head of the fjord with crest-to-trough height up to 80 cm. The oscillations in Vestfjorden are clearly identified for the entire period 29–31 October. North of the Lofoten Islands at Harstad and Andenes the signal is weaker and hardly identifiable.

The northward propagation of the signal along the west coast of Norway can be followed by tracing a particular phase at the front of the main group of oscillations. This is identified as a clearly defined first peak between 27 and 28 h at Stavanger, at 28–29 h at Bergen, and at about 29 h at Måløy. The same peak can also be identified on the records from stations further north along the coast. The travel time of this peak and computed phase speeds between some stations between Bergen and Bodø are listed in Table 2.

The results show that the speed of propagation varies considerably along the coast with the phase speed from 34 ms^{-1} to 107 ms^{-1}. The error in this estimate is, however, large since the propagation time is relatively short compared to the period of the individual waves. Numerical calculations of the phase speed for a baro-

Table 2 Travel time, distances, and phase speed

Station	Travel time (min)	Distance (km)	Speed (ms^{-1})
Bergen	0	0	
			107
Måløy	28	180	
			34
Kristiansund	126	378	
			85
Rørvik	174	624	
			65
Bodø	253	933	

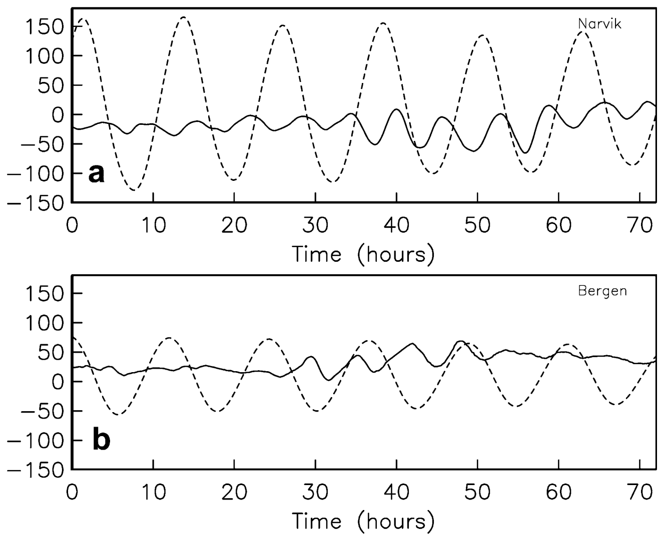

Fig. 7 Predicted astronomical tide (in cm) for Bergen and Narvik (*broken lines*) and observed residual sea-surface displacement (*full lines*). Time origin 00 UTC 29 October 2000

tropic Kelvin wave with period 6 h for various sections of the west coast of Norway show phase speed ranging from 85 to 135 ms^{-1} depending on the shelf sea depth and the width of the shelf. It therefore seems that the observed propagation speed for the signal is somewhat lower than the speed of a barotropic Kelvin wave with the same period. The reason for this may be partly due to the effect of the numerous large fjords along the coast; each of them may cause a delay of the wave, as shown by Miles (1972). Friction may also have an additional delaying effect.

In order to demonstrate that the oscillations are not phase-locked to the tide, the predicted astronomical tide and the residual signal are shown for two stations, Bergen and Narvik, in Fig. 7.

5 Model simulations and comparison with data

The performance of British operational storm surge model CS3 (see Sect. 3) during the late October 2000 event has been studied by Flather and Williams (2001). It predicts the surge oscillations reasonably well for most British stations, as well as the oscillations with 12-h period observed in Skagerrak (see Sect. 4). The rapid changes in surge elevation and timing errors caused significant errors at some places. The 6-h oscillations at Stavanger and Bergen in southwestern Norway are also predicted by the model, although these stations are located near the northern boundary of the model domain and a close resemblance with observations cannot be expected. Actually, the agreement is best for Stavanger, while the prediction for Bergen shows some phase errors.

Animations of the sea-level variation in the northeastern North Sea based on data from the CS3model show that oscillations with about 6-h period appeared in the southern North Sea and propagated northeastward along the coast of The Netherlands and into the German Bight. Similar oscillations also appeared in the area southwest of Stavanger, where localized small-scale variations in the wind-stress field occurred (Figs. 3, 4). A sequence of color contour maps of the residual sea-level displacement in the North Sea from 30 October 2000 is presented in Fig. 8. It shows a complex pattern of rather large-scale sea-level disturbances where the quarter-diurnal signal is superimposed, but not so easily identifiable. We have also filtered the sea-level displacements field with a low-frequency band pass filter with cutoff around 8 h. The filtered sea level is then subtracted from the original signal to obtain a filtered signal containing the quarter- diurnal oscillations. When plotted, these filtered fields (not shown) display clearly the quarter-diurnal signal propagating northeastwards along the coast of The Netherlands and into the German Bight. It was not possible, however, to identify these oscillations in the filtered time series from the three stations Hirtshals, Tregde, and Helgeroa, and follow the propagations across Skagerrak.

To study the effect of nonlinear tide–surge interaction we ran the CS3 model both with and without tides. Figure 5 shows the detided prediction (i.e., astronomical tide removed after the simulation) for some stations in the northern and northeastern part of the North Sea. Also shown is the difference between the detided model simulations and the model results without tidal forcing. The difference (fine dotted lines in Fig. 5) gives an indication of the tide–surge interaction. The interaction effect at the three stations Hirthals, Helgeroa, and Tregde appears as oscillations with nearly semidiurnal period and crest-to-trough height up to 0.5 m. At Stavanger and Lerwick further west the interaction does not contain any noticeable oscillations with 6-hour period. At Wick on the coast of Scotland (Fig. 5) the tide produces by nonlinear interaction O(10 cm) amplitude oscillations with 6-h period. This leads to the conclusion that the large 6-h oscillations observed in the northern part of the North Sea are mainly due to the atmospheric forcing.

As expected, the results of the simulations with the 12.5-km resolution NBS model (see Sect. 3) show a northward-propagating wave signal along the western coast of Norway. The wave energy is mostly confined to the shelf zone with depth less than 500 m (Fig. 1). The waves have the character of coastal trapped waves with wave length of about 900 km modified by bottom topography and the geometry of the coastline. In the north, at about 68°N, the waves are scattered by the Lofoten Islands, where the shelf width narrows to less than 50 km. North of the islands the wave signal is very weak. In the large bay area south of the islands, Vestfjorden, the waves are amplified. This agrees qualitatively well with the observations (see Sect 4).

In order to study the local wave transformation near the Lofoten Islands in more detail, we performed addi-

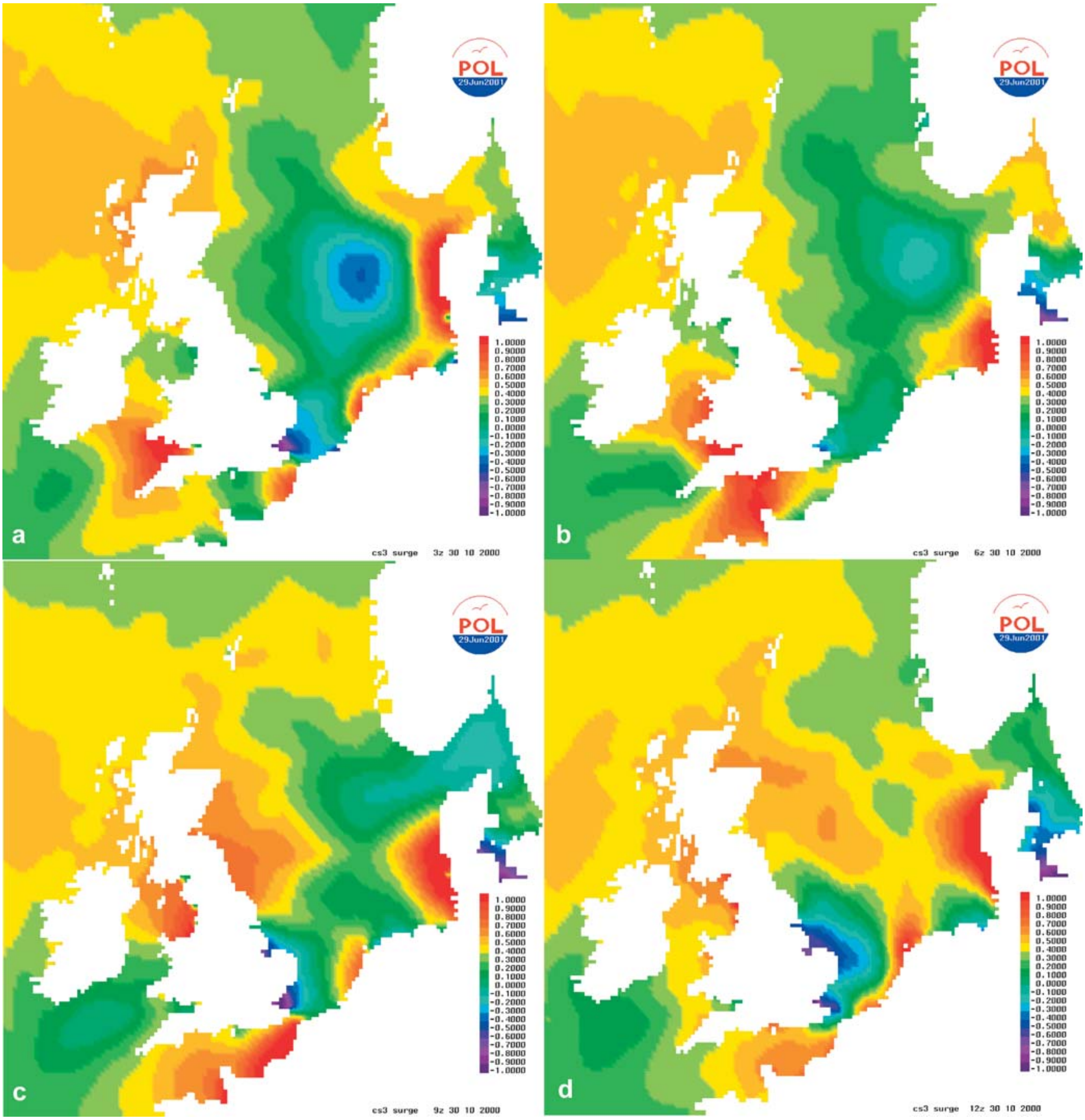

Fig. 8a–d Colour contour maps of residual sea-level displacement (tide-removed) in the North Sea from the CS3 model on 30 October 2000 at 3, 6, 9, and 12 UTC panel **a–d** respectively

tional model simulations with the HRN model. The location of the model domain is shown on the overview map in Fig. 1 and the details of the bathymetry for the model domain as displayed in Fig. 9. A wave input of the form Eq. (1) is applied along the southern boundary of the model with peak amplitude at the coast (170 km) decreasing linearly to zero at the southwestern corner of the model (0 km). Along the western and northern boundaries radiation conditions are implemented. In Fig. 9 the contour lines for sea-level displacement at $t = 27$ h clearly show the amplification of the wave in Vestfjorden, the bay area south of the Lofoten Islands. We note that the sea level increases gradually from the mouth of the fjord south of Værøy (V in Fig. 9), indicating a co-oscillating type of mode in the fjord (see below)

The variation in wave amplitude in the area is also seen by the time series for sea-level displacement at these five stations: Bodø (Bo), Kabelvåg (Ka), Narvik (N), Harstad (Ha), and Andenes (A) (Figs. 9,10). Time-series

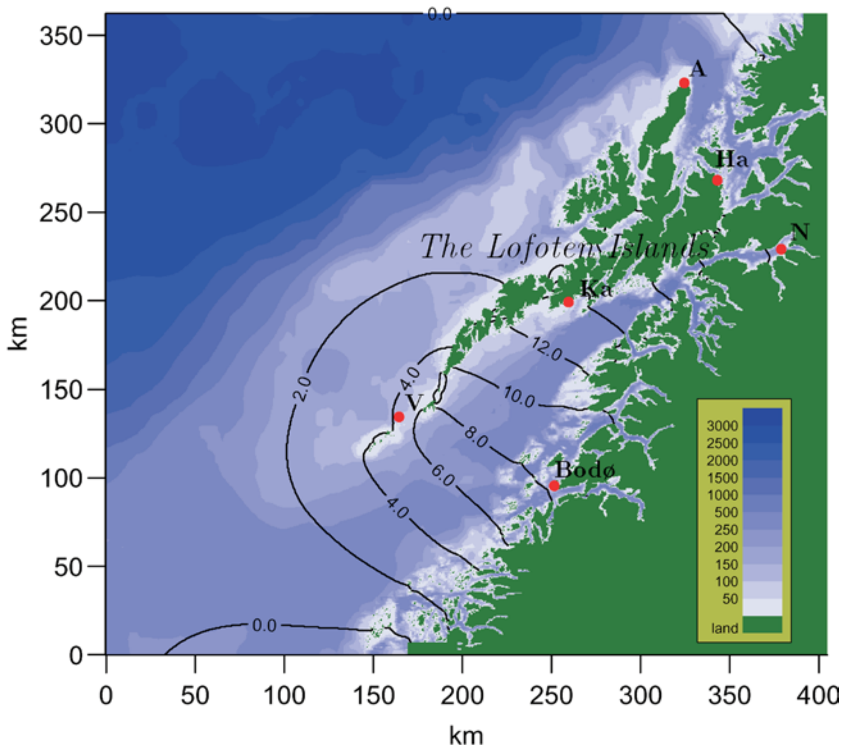

Fig. 9 Contour lines for sea-surface displacement (intervals 2 cm) at $t = 27$ h with wave input at southern boundary (see text). Location of Bodø, Narvik (*N*), Kabelvåg (*Ka*), Harstad (*Ha*), Andenes (*A*), and Værøy (*V*) are shown. For the latter station only model data. Colors indicate water depth in meters

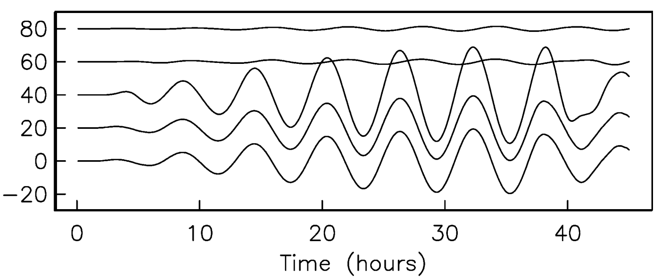

Fig. 10 Time series of modeled sea-surface displacements for stations in the Lofoten area; Bodø, Kabelvåg (Ka), Narvik (N), Harstad (Ha) and Andenes (A), ordered *from bottom to top*. The graphs are successively displaced by 20 cm to avoid overlap

for sea-level displacement from a station near Værøy (V) west of Lofoten (not shown in Fig. 10) confirms that the largest amplitude is confined to the Lofoten bay (Vestfjorden). Despite the fact that the exact cross-shelf structure of the wave at the southern boundary of the model is unknown, the amplitude variation is qualitatively in good agreement with the observations (Fig. 6). Simulations with wave period $t_p = 4$ h show an even sharper amplification peak at Narvik, while with period $t_p = 8$ h the amplification effect is reduced and the oscillations are noticeable also at the two stations Harstad and Andenes north of the Lofoten Islands. Amplification of the semidiurnal and the diurnal tide around the Lofoten Islands has been demonstrated by Moe et al. (2002) and related to the topography of the shelf and the coastline.

The local wave amplification observed in Trondheimsfjorden is investigated by the HRS model (see Sect. 3). The fjord proper is about 135 km long, 8–30 km wide and with depth to about 600 m. The location of the model domain is shown on the overview map in Fig. 1 and the details of the bathymetry for the model domain are displayed in Fig. 11. A wave input of the form Eq. (1) is applied along a section of the western boundary of the model with peak amplitude at the coast (45 km) decreasing linearly to zero 150 km from the southwestern corner of the model domain. Along the remaining section of the western boundary and on the northern boundary, radiation conditions are implemented. The overview, (Fig. 11), displays the contour lines for sea-level displacement at $t = 27$ h in the Trondheimsfjorden area. The amplification within the fjord is shown by by an enlargement, (Fig. 12), with wave amplitude increasing from about 8 cm at the mouth to more than 32 cm at the head of the fjord.

The variation in wave amplitude in the area is also seen by the time series for sea-level displacement at five locations: Kristiansund, Heimsjø (He), Trondheim, the inner Trondheimsfjord (Be), and Rørvik (Figs. 11–13). Although the exact cross-shelf structure of the wave at the western boundary of the model is unknown, the amplitude variation is qualitatively found to agree well with the observations (Fig. 6). A considerable amplification takes place inwards from Trondheim, as seen from the time series for a location (Be) at the head of the fjord, but no observations are available to confirm this finding. Additional simulations with the period of the input wave signal $t_p = 4$ h and 8 h show that the amplification has a rather sharp peak around $t_p = 6$ h. An amplification of the sem-

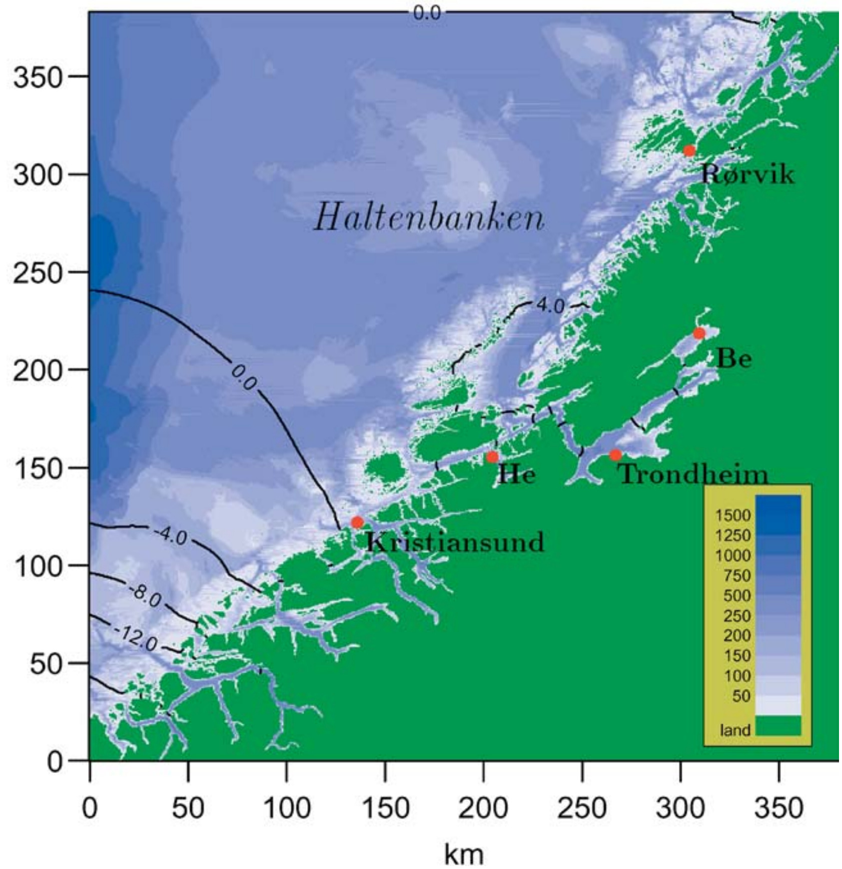

Fig. 11 Contour lines for sea-surface displacement mid-Norway (intervals 4 cm) at $t = 27$ h with wave input along the western boundary (see text). Location of Kristiansund, Heimsjø (*He*), Trondheim, inner Trondheimsfjord (*Be*) (only model data), and Rørvik are shown. Colors indicate water depth in meters

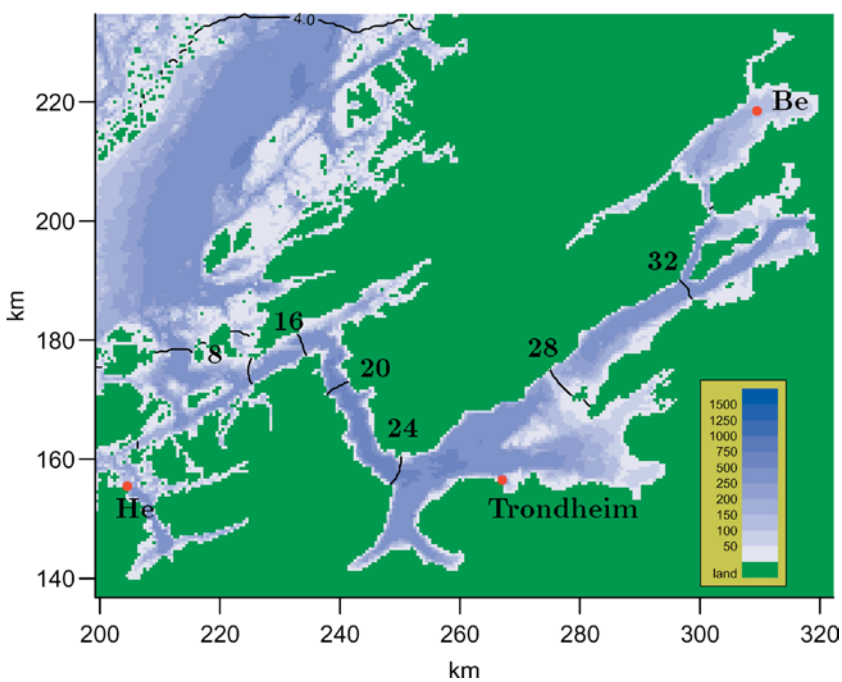

Fig. 12 Enlargement of Trondheimsfjorden from Fig. 11. Contours for sea-level displacement with 4-cm intervals. Colors indicate water depth in meters

idiurnal tide (M_2) with an amplitude increase of about 15 cm from the mouth to the head of the fjord was reported by Moe et al. 2003.

The observed local amplification of the signal in the two fjord systems, Vestfjorden in Lofoten, and Trondheimsfjorden, can be explained in terms of a co-oscil-

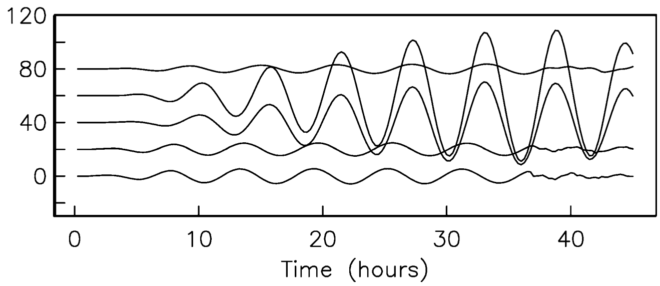

Fig. 13 Time series of modeled sea-surface displacements for stations in mid-Norway; Kristiansund, Heimsjø (He), Trondheim, inner Trondheimsfjord (Be), and Rørvik ordered *from bottom to top*. The graphs are successively displaced by 20 cm to avoid overlap

lating mode where the water in the fjord communicates with the open ocean through the fjord mouth. The term Helmholtz mode is also used for this type of oscillation (Miles 1974, and references therein). For the simple case of an open rectangular fjord of length L and uniform depth h connected to a deep ocean, the period is $T = \frac{4L}{\sqrt{gh}}$. A crude approximation for Vestfjorden is $L = 260$ km and $h = 400$ m, leading to $T = 4.6$ h. An equivalent length for Trondheimsfjorden is more difficult to estimate due to the complex coast form and the islands outside the fjord, but may be somewhat larger than the length of the fjord proper. If we take $L = 150$ km and mean depth $h = 500$ m we obtain $T = 2.4$ h. A mouth correction factor may apply here, bringing the period closer to 6 h. Clearly, the depth and width of the shelf outside the mouth will influence the period as well as frictional effects and the Earth's rotation, but these effects can only be estimated by numerical simulations with realistic high-resolution fjord and shelf bathymetry, as shown by the examples above.

6 Conclusions

This study investigates a special storm situation 29–31 October 2000 which led to long regular trains of residual sea-level oscillations with 6-h period in the North Sea. The oscillations were recorded over a large area from Dover in the English Channel to Lofoten in northern Norway. In Skagerrak in the northeastern part of the North Sea the main storm-surge signal had a character of amplitude-modulated oscillations with period about 12 h and crest-to-trough height up to 1.5 m. Along the western coast of Norway, outside the central storm area, long trains of regular oscillations with period about 6 h and crest-to-trough height up to 0.8 m were observed. Simulations with the British operational storm-surge model (CS3) show that the latter oscillations most likely were generated by rather small-scale spatial and temporal variations in the wind-stress field localized to the area off the coast west of Stavanger, southern Norway.

The sea-level oscillations propagated northwards along the coast of Norway as coastal trapped waves and were amplified locally in some fjords, notably in Trondheimsfjorden, mid-Norway, and in Vestfjorden in the Lofoten area. The wave amplification in these fjords and the scattering of the wave signal by the Lofoten Islands are also confirmed by simulations with high-resolution local models.

The train of oscillations with 6-h period were also recorded at stations along the eastern coast of Scotland and at Lerwick on Shetland. The signal from Lerwick correlates with the signal recorded at Bergen on the Norwegian coast east of Shetland.

Model simulations with the CS3 surge model with and without tides included show that the oscillations with period about 6 h in the northern North Sea and along the west coast of Norway is little affected by nonlinear tidal effects or tide–surge interaction. An exception is Wick on the east coast of Scotland, where the tide produces small amplitude oscillations with period about 6 h. The tide–surge interaction is, however, noticeable at stations in Skagerrak in the northeastern North Sea, particularly at Hirtshals, Helgeroa, and Tregde, where the interaction produces a significant semi-diurnal signal. The 6-h oscillations are not detected in Skagerrak. At stations along the coast of England in the southern North Sea and in the English Channel, oscillations with 6-h period are partly due to nonlinear effects and small-scale variations in the wind stress. The oscillations propagate northwards from the English Channel along the coast of The Netherlands and Germany and can be traced in the observations from Esbjerg on the southern coast of Jutland, Denmark (Fig. 5). There is a close correlation between the oscillations at Esbjerg and Bergen (see Sect. 4), but we have not been able to follow the propagation of the signal between these two stations.

The storm of 29–31 October 2000 seems to be a rare event, but we have not systematically examined archive data to identify other similar events. The amplitude of the observed oscillations is so large that the phenomena is of practical significance although it is not a frequent event.

Acknowledgements The authors are grateful to the Danish Meterological Institute and Faroese Office of Public Works for providing sea-level data and to Alan M. Davies for commenting on the draft manuscript.

References

Andersen OB (1999) Shallow-water tides in the Northwest European Shelf region from Topex/Poseidon altimetry. J Geophys Res 104: 7729–7741

Davies AM, Lawrence J (1994) Modelling the non-linear interaction of wind and tides: its influence on current profiles. Int J Numer Meth in Fluids. 18: 163–188

Davies AM (1986) A three-dimensional model of the Northwest European Shelf with application to the M_4 tide. J Geophys Res 16: (5) 797–813

Davies AM, Jones JE (1996) Sensitivity of tidal bed stress distribution, near-bed currents, overtides and tidal residuals to fric-

tional effects in the eastern Irish Sea. J Phys Oceanogr 26: (12) 2553–2575
Flather RA (2000) Existing operational oceanography. Coast Eng 41: 13–40
Flather RA, Williams JA (2001) Investigation of the operational model performance during 2000/01. Proudman Oceanographic Laboratory, UK. Internal document No. 139, 16 pp
Gjevik B, Nøst E, Straume T (1994) Model simulations of the tides in the Barents Sea. J Geophys Res 99: (C2) 3337–3350
de Jong MPC, Holthuijsen LH, Battjes JA (2003) Generation of seiches by cold fronts over the southern North Sea. J Geophys Res 108: (C4) 14-1 - 14–10
Kwong SCM, Davies A, Flather RA (1997) A three-dimensional model for the principal tides on the European shelf. Prog Oceanog C2 3: (3) 205–262
Miles JW (1972) A note on tidal delay by inland seas and harbors. Geophys Fluid Dynam 3: 27-34
Miles JW (1974) Harbor seiching. Ann Rev Fluid Mech 6: 17–35
Moe H, Ommundsen A, Gjevik B (2002) A high, resolution tidal model for the area around the Lofoten Islands, northern Norway. Continental Shelf Res 22: 485–504
Moe H, Gjevik B, Ommundsen A (2003) A high-resolution tidal model for the coast of Møre and Trøndelag, western Norway. Norw J Geog 57: 65-82
Pingree RD, Griffith DK, Maddock L (1984) Quarter-diurnal shelf resonance and tidal bed stress in the English Channel. Continental Shelf Res 3: (3) 267–289